No Watt Left Behind

Academic and Research Staff
Professor Steven B. Leeb

Graduate Students
John J. Cooley, EECS, Al Avestruz, EECS, Warit Wichakool, EECS, Zachary Remscrim, EECS, Christopher Schantz, ME, James Paris, EECS, Sabrina Neuman, EECS, Darin Barber, EECS and ME, Uzoma Orji, EECS, Daniel Vickery, EECS

Undergraduate Students
Mike Ciuffo, EECS, Julie Hui, Physics, Jose Cruz, EECS

Technical and Support Staff
Denise Stewart, Administrative Assistant

1. No Watt Left Behind

Sponsors
U.S. Navy Office of Naval Research
U.S. Coast Guard
U.S. Department of Energy
The Grainger Foundation

Project Staff
J. Cooley, D. Vickery, A. Avestruz, J. Paris, Z. Remscrim, U. Orji, D. Barber, S. Neuman, and S. Leeb

At any point in the life of a building, mechanical and electrical equipment – the services infrastructure – may be poorly operated. Equipment may be inadvertently left in operation when not needed: lights and fans running all night or air conditioning in unoccupied spaces. Or equipment may be operated in ignorance of the cost, a problem exacerbated by time-varying electrical rates. Further, as buildings age, both the equipment and the building façade or envelope – a part of the construction infrastructure – wear, cease to function properly, and eventually fail, via myriad processes that are often undetected. Valves do not close fully, dampers stick, refrigerant leaks, heating and cooling coils – from the smallest refrigerator to the largest building air-conditioning system – become fouled with accumulated dirt and debris, and belts slip.

As we enter a new round of contemplation about adding information gathering and control capability for managing grid demand, it is imperative that we consider the results of previous forays. Much of the current thinking for making buildings “smart” about their energy consumption recapitulates old ideas with new technological varnish. Computational power and data transmission capabilities for commercial monitoring and control systems have out-paced the problem of putting sensors in all the right places. Various kinds of high-speed data networks provide convenient remote access to control inputs and system operating information for embedded control and monitoring systems. Similarly, microprocessors and associated technologies for these systems have achieved astounding price/performance ratios. Obtaining useful information, however, generally requires proper installation, maintenance, and interpretation of a vast collection of sensors – a daunting proposition even if the sensors are mass produced, micro-miniature, and individually inexpensive.

Facilities managers for industrial and commercial sites want to develop detailed consumption profiles for utility services like electricity, water, and gas consumed in their buildings. This information is essential in order to understand and optimize energy consumption, to detect and

solve equipment failures and problems, and to facilitate predictive maintenance of various utility loads. As electrical, gas, and water costs rise, residential customers are also developing a growing interest in understanding the magnitude and impact of their consumption quickly, easily, and informatively.

Conventional sub-metering of utility services to detect problems and conduct energy and consumption score-keeping has long been costly and inconvenient. For electrical consumption, for example, a nagging problem for over two decades has been that these costs increase swiftly as data requirements become increasingly complex. There is a need, for example, for flexible, inexpensive metering technologies that can be deployed in many different monitoring scenarios. Individual loads may be expected to compute information about their power consumption. They may also be expected to communicate information about their power consumption through wired or wireless means. Switch gear like circuit breaker panels may soon be expected to provide detailed submetering information for different loads on different breakers or clusters of breakers and controls. New utility meters will need to communicate bidirectionally, and may need to compute parameters of power flow not commonly assessed by most current meters.

The U.S. Department of Energy has identified “sensing and measurement” as one of the “five fundamental technologies” essential for driving the creation of a “Smart Grid”. Consumers will need “simple, accessible. . . , rich, useful information” to help manage their electrical consumption without interference in their lives. Both vendors and consumers will likely find innumerable ways to mine information if it is made available in a useful form. However, appropriate sensing and information delivery systems remain a chief bottleneck for many applications, and metering hardware and access to metered information will likely limit the implementation of new electric energy conservation strategies in the near future.

We are inventing new ways to collect utility usage data with a greatly reduced investment in sensors. Our “non-intrusive” approach can determine the operating schedule of a collection of electrical loads from a single measurement of aggregate current flowing to the loads. It can also determine the precise location of water consumption from a single acoustic measurement at the building water main. The nonintrusive utility monitor addresses the “sensor problem” for by extracting information about individual loads, e.g., a fan, a computer, a light, a sink, a shower, etc., from limited measurements at an easy-to-access, centralized location. For example, the nonintrusive monitor can disaggregate and report the operation of individual electrical loads like lights and motors from measurements made only at the electric meter where service is provided to a building. The nonintrusive monitor is capable of performing this disaggregation even when many loads are operating at the same time. Because the monitor associates observed electrical and acoustic waveforms with individual kinds of loads, it is possible to exploit modern state and parameter estimation algorithms to remotely verify and determine the condition or health of critical loads

Our “No Watt Left Behind” initiative is a broad ranging look at the way electro-thermal-mechanical systems used energy in buildings, with an eye toward advanced technology demonstrations in intelligent lighting, power electronics, waste heat recovery, metering, and control. A (not exhaustive) list of example projects is presented below:

1.1 Signal Processing Hardware

For electrical monitoring, the nonintrusive approach makes measurements of voltage and current solely at the utility service entry of a building, as shown in Figure 1. It characterizes individual loads by their unique signatures of power drawn from the mains. A transient detection algorithm can identify when each load turns on and off, even when several do so nearly simultaneously.

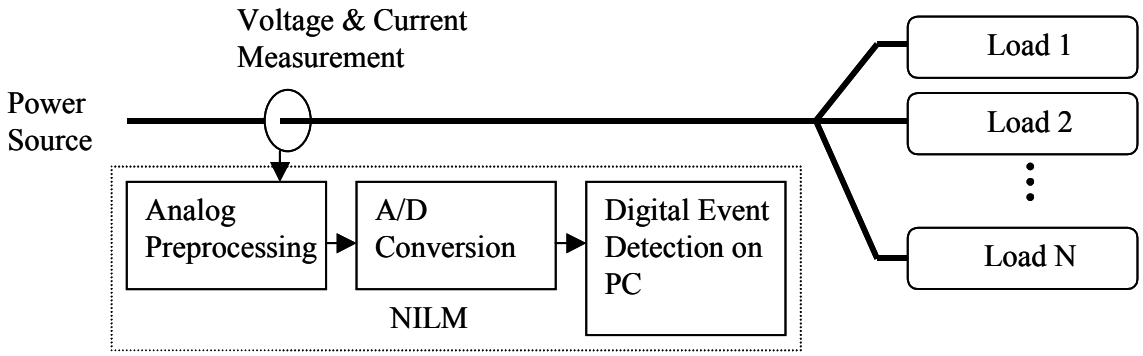

Figure 1: Block Diagram of Non-Intrusive Load Monitor

Figure 2 shows a photograph of the prototype hardware that we have developed and deployed during our tests. This FPGA-based preprocessing unit observes voltage and current, and computes the spectral envelopes that serve as the signal processing basis for nonintrusive electrical load monitoring. The details of this signal processing are described below.

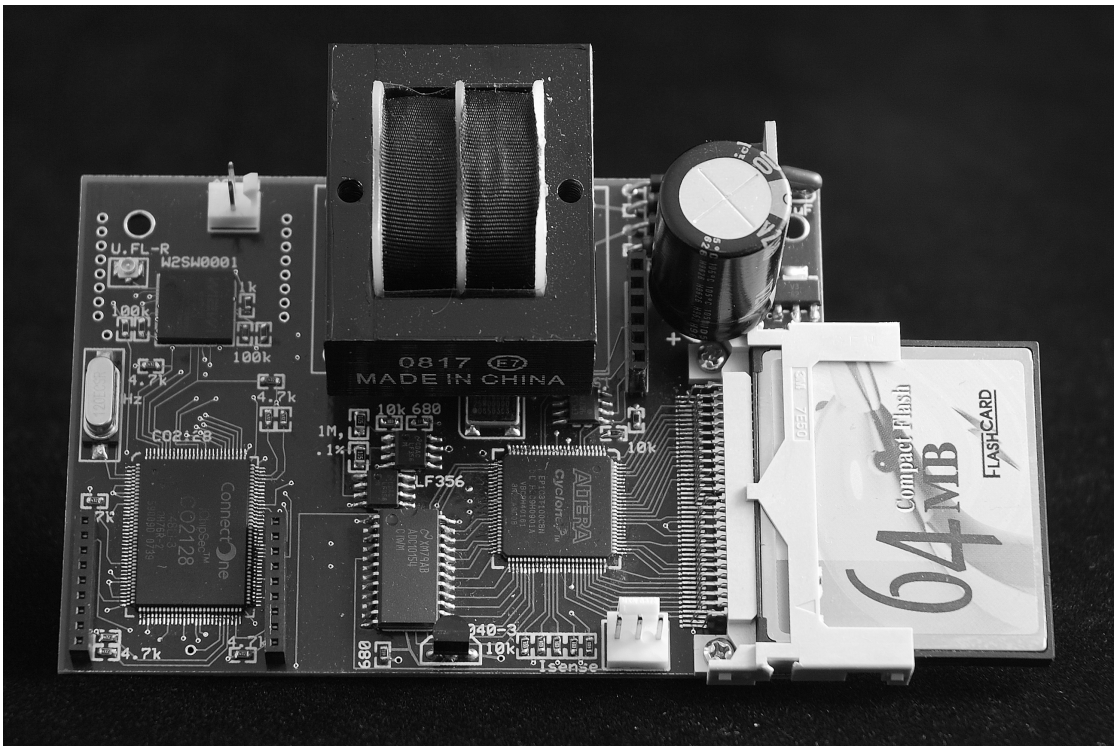

Figure 3 shows a screen print from our prototype, real-time, load monitor. The preprocessor shown in Figure 2 communicates wirelessly with a personal computer running our prototype monitoring software. The screen capture in Figure 3 is from a personal computer in communication with the preprocessor board. Two loads, an incandescent lamp and a motorized tool are shown activating in Figure 3. As shown in Figure 3, once trained with fingerprint signatures for the loads to be identified, the prototype event detector is able to recognize the turn-on transients ("exemplar 1 and exemplar 2") of both loads strictly by examining the aggregate traces of real power, reactive power, and harmonic content at the service entry.

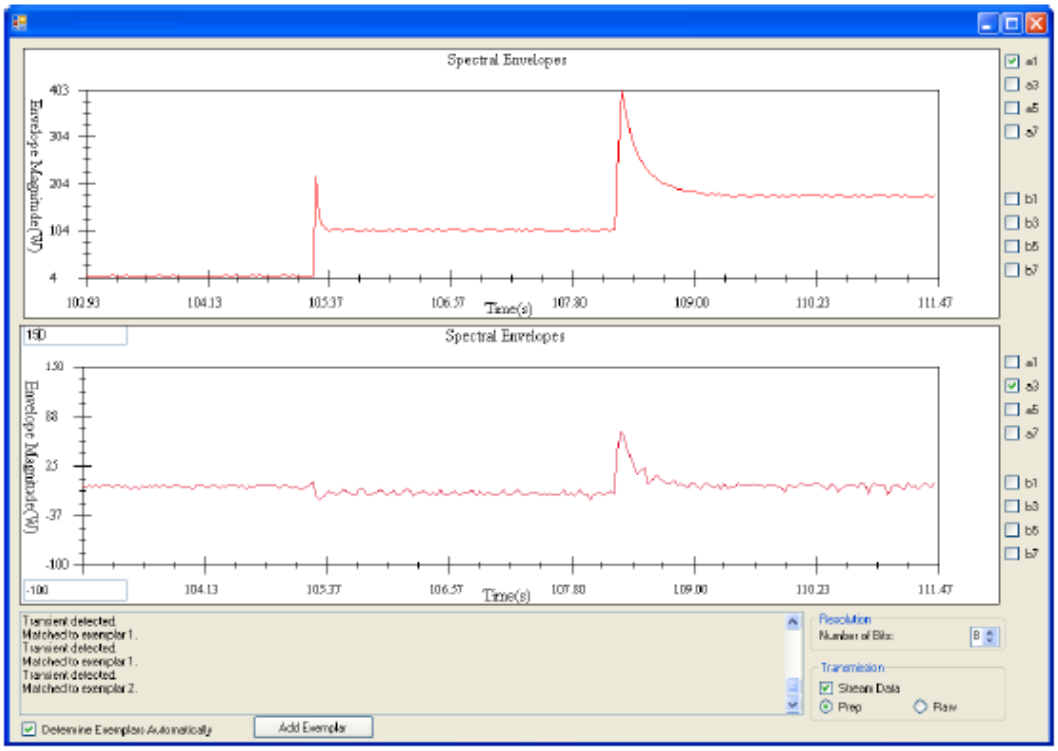

Figure 3: Screen capture from personal computer in WiFi communication with the Figure 2 preprocessor board.

We have confirmed that direct examination of current or acoustic waveforms may not be the best choice for many stages of some monitoring and control applications, including many components in energy scorekeeping, monitoring, or conservation systems. Direct operations on the current waveform require sample rates adequate to capture the highest harmonic content of interest [12]. In some metering, monitoring, and control applications it is more practical either to store data for a period of time and examine it later, or to transmit data to another location for interpretation and control. In either of these cases, it is convenient to have a useful representation of the data that avoids excessive storage or communication bandwidth requirements. We have designed and deployed an FPGA-based signal processing device that can compute spectral content for observed waveforms, including electrical current and hydrodynamic acoustic signatures. This FPGA serves as the core of a new information appliance, a nonintrusive monitor that can track and disaggregate all utility consumption in a building from a very small sensor set.

Spectral envelopes represent the time-varying harmonic content of waveforms, e.g., observed current waveforms. Spectral envelopes are illustrated in the graphs in Figure 3 for the currents consumed by the associated loads. They provide a useful separation between data collection and analysis. They will permit a small, inexpensive system with low processing power to collect data continuously. A system with larger available processing power, potentially physically remote from the data collection front-end, can either review a storage device at a later time or continuously process a relatively low bandwidth information stream over a convenient communication channel, wired or wireless.

To calculate, store, and communicate a relevant subset of DFT coefficients for power monitoring and energy scorekeeping, a prototype FPGA (Field Programmable Gate Array) was constructed to implement a spectral envelope preprocessor. This system makes use of a low-cost FPGA

(Altera Cyclone I, EP1C3T100C8). The spectral preprocessor consists of four subsystems: a subsystem that obtains current and voltage samples, a subsystem that computes spectral envelope coe_cients, a subsystem that stores computed spectral envelope coefficients, and a subsystem that can transmit the spectral envelope coefficients to another computation or display platform for further analysis. Each of these subsystems will be considered in detail. Figure 4 shows the overall block diagram of the system.

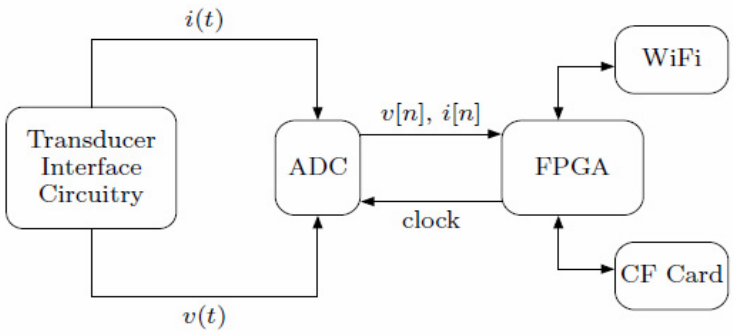

Figure 5: Spectral envelope pre-processor block diagram

Data flows through the system as follows. The transducer interface circuitry measures the line voltage and aggregate current, producing the signals v(t) and i(t). These signals are sampled and quantized by an analog-to-digital converter (ADC) that produces the samples v[n] and i[n]. The FPGA processes these samples to compute spectral envelopes. The spectral envelope coefficients can be stored in a Compact Flash (CF) card for later use. The system also includes an 802.11b/g WiFi transceiver that allows any collection of the spectral envelope coefficients to be transmitted to another computation device for analysis. The FPGA provides control logic for each of the subsystems.

Current and voltage measurements from at least one voltage channel and at least one current channel are used to compute spectral envelopes. The system is easily expanded to measure more than two channels, supporting three-phase electrical services, for example. The prototype system uses an LA-55 current transducer to measure aggregate current and a transformer to measure the line voltage. A transformer with dual secondary coils was used in the prototype. This provides one coil for measurement purposes, and a second coil for powering the preprocessor. The two coil arrangement provides a voltage sense with very little phase distortion, ensuring accurate calculation of in phase and quadrature spectral components.

In many signal processing applications, a computationally efficient algorithm like the Fast Fourier Transform (FFT) computes the complete spectral analysis of a sampled waveform. However, in situations like power monitoring, where a relatively small number of spectral coefficients may contain all or most needed information, needed spectral coefficients can be computed more efficiently by a traditional DFT implementation, i.e., by mixing observed waveform samples directly with the stored samples of basis sinusoids. In this approach, basis sinusoids are stored in a memory and multiplied by observed samples of a waveform. If there are N samples stored in memory for each basis sinusoid, then it is necessary to acquire N samples of the current and voltage waveforms for each line voltage period.

The FPGA coordinates the operation of the ADC (Analog to Digital Converter) to obtain the samples i[n] and v[n] of the current and voltage waveforms i(t) and v(t). To provide a known number of waveform samples per line period, the FPGA “locks" to the line-voltage waveform.

That is, the FPGA varies the sample rate to track with variations in the line voltage frequency. The sampling clock is derived from the output of a digital phase-locked loop (PLL) on the FPGA that tracks the line voltage frequency. The phase of the sampling is set such that the firrst voltage and first current samples are taken at the negative to positive zero crossing of the line voltage. The goal is to multiply each entry in the basis sinusoid by the value of the waveform to be analyzed at the corresponding point in time. It is essential that the entire process is line locked to the line frequency in order for the estimated spectral envelope coefficients of current to correspond to “in-phase" and “quadrature" components of current with respect to the fundamental of the voltage waveform.

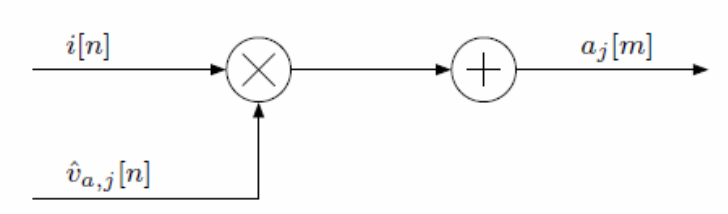

Figure 6: Computation of a spectral envelope

The FPGA computes spectral envelopes using integer arithmetic on stored basis waveforms and observed waveform samples. The FPGA-based spectral envelope preprocessor calculates the spectral envelopes of current, a1[m], b1[m]…, where m indexes the periods of the line voltage. Figure 5.9 shows the computation performed to produce estimates of a single spectral envelope coefficient, $a_j[m]$. The system multiples i[n], the samples of current, with $v_{a,j}$ [n], the samples of a basis sinusoid, and sums the result over a single period of the line voltage.

Each spectral envelope coefficient has a different basis sinusoid associated with it; for example, calculation of a3[m] involves multiplying i[n] by discrete time samples of a sinusoid at three times the line frequency, with its phase locked to the line voltage. Figure 7, shown below, depicts examples of basis sinusoids. For illustration purposes, these sinusoids are sampled at only 3 bits, while the prototype system makes use of 10 bit samples.

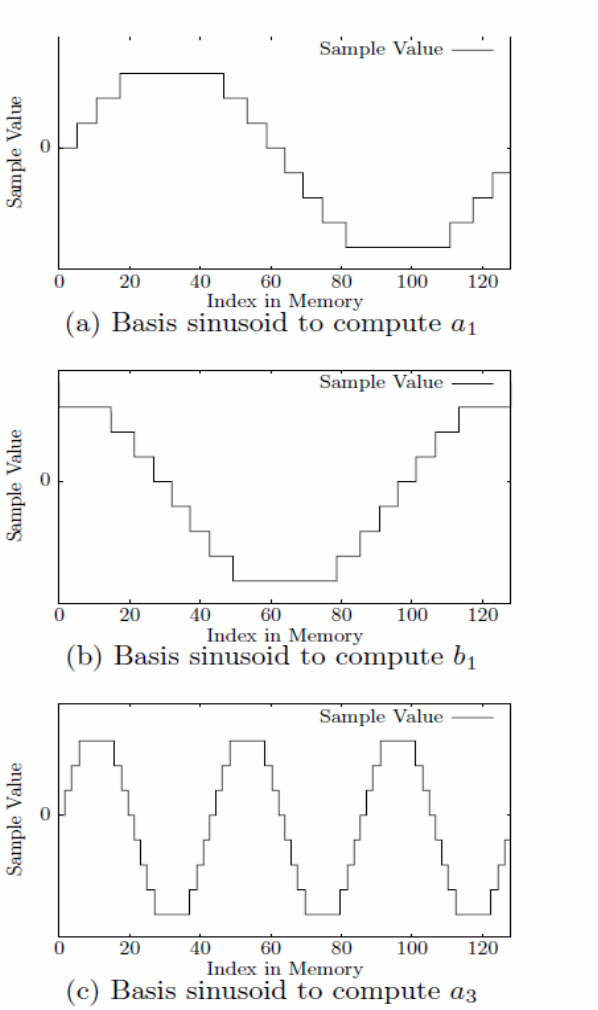

Figure 7: Low-resolution (illustrative example) basis sinusoids

This implementation is also efficient in terms of FPGA resource utilization. It uses only a single PLL and a single multiplier. This system can function with only a single multiplier because the FPGA is capable of multiplying each sample i[n] by the corresponding sample of each of the basis sinusoids and forwarding each result to the appropriate accumulator, before the next sample i[n + 1] arrives. The multiplier consumes substantial logic elements on the FPGA. It consumes 24% of all resources used by the envelope preprocessor and 13% of all resources used by the complete system. By using only one multiplier, the design is capable of fitting in a small, low-cost FPGA.

Spare capability on the FPGA subsystem is used to control the storage of spectral envelope data on an erasable memory like a CF (Compact Flash) storage card. This subsystem is capable of storing spectral envelope data as it is produced, as well as retrieving the spectral envelope data from any point in time, on demand. The FPGA also control the operation of a WiFi interface, which can be used to retrieve data in real time. The current design is capable of supporting both ad-hoc and access point (infrastructure) networks. The transmitted data is retrieved from the CF card as needed. The WiFi subsystem can operate in two different modes. In the first mode, the system streams spectral envelope coefficients as they are generated. In the prototype, this corresponds to a data rate of 2:8 KB/s. In the event of a momentary interruption in the connection

to the PC, the system will automatically buffer data from the last successfully transmitted packet and resume transmission from that point when a connection is reestablished. The system will then send data at the highest available transmit speed (54 Mb/s for 802.11g), until the system catches up to the freshly produced spectral envelope data. In the second mode, an application on the PC requests data by specifying a range of time; the system then transmits all data from the desired range of time, at the maximum possible transmission speed.

The FPGA-based system discussed above calculates, stores, and transmits spectral envelope data. Figure 2 shows a picture of the prototype hardware. To make use of this data, a monitoring or control system typically includes a subsystem to receive and use the spectral envelope data. For example, a homeowner could use a personal computer to collect spectral envelope data from the FPGA preprocessor installed near or in a circuit breaker panel. The prototype includes a PC-based software application that can interface with the FPGA-based preprocessor via wired or wireless communication channels, retrieve spectral envelopes, and display spectral envelope data. This PC-based interface was used to collect the screen capture shown in Figure 3 from the operating prototype.

1.2 Retrofit electrical sensor

Closed or “clamp” core sensors wrapped around the utility feed typically provide the current sense signal for a nonintrusive monitor. These sensors prohibit widespread monitoring because skilled labor must separate Line and Neutral in order to deploy a wrap-around magnetic field sensor, even in the case of separable core sensors. We have demonstrated an alternative to traditional clamp or Hall-effect sensors. This alternative requires no skilled installation. This new sensor measures the current in the utility feed by sensing the resulting magnetic field at the face of the main (or other) circuit breaker in a standard breaker panel, where the Line and Neutral are already separated. The sensor can be interrogated through the steel panel door with no direct electrical contact, as the door must be closed to comply with safety regulations. Our connection to the front face of a circuit breaker is shown schematically on the left in Figure 8. The photograph on the right in Figure 8 shows the internal mechanism of a typical circuit breaker. The convoluted path of current through the protection gear inside the breaker makes a magnetic field that can be detected without electrical contact outside of the plastic breaker face. While breakers differ slightly in construction, our survey of dozens of commercial breakers indicates that this approach will work with little or no modification in most circuit breaker panels in at least North America.

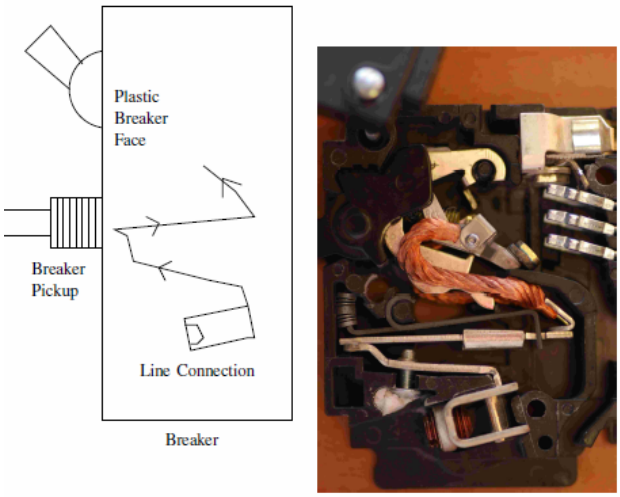

Figure 8: Circuit breaker pickup and typical circuit breaker (opened for illustration).

A schematic of our preliminary test apparatus to verify the concept is shown in Figure 9, employing a spectrum analyzer and signal generator. The circuit breaker and circuit breaker pickup coil are shown schematically at the far right in Figure 9. The circuit breaker pickup is small and fits between the panel door and the front face of the breaker. The complete sensor shown in Figure 4 consists of three main parts: an inductive pickup for sensing current from the breaker face (Breaker Pickup), an inductive link designed to transmit power through the steel breaker panel door (Through-door Inductive Link), and a balanced JFET modulator circuit for transmitting information through that inductive link (JFET Mixer).

The outer coil is driven with a high-frequency sinusoidal carrier voltage. That voltage couples to the inner coil through the inductive link and drives a new JFET mixer. The JFET mixer controls the amount of current drawn from the inner coil, modulated by the low-frequency (60 Hz) current signal measured by the breaker pickup. The result is a modulation between the high frequency carrier signal and the low-frequency (60 Hz) signal measured at the breaker face. The external sense circuit monitors the current drawn through the inductive link to extract the resulting modulated signal. The internal device is fully powered by the applied carrier, and the entire system works without modification to the breaker panel or the circuit breaker itself. With the modulated signal available to the sense circuit external to the door, the current through the main breaker can be analyzed by the nonintrusive monitor for load identification and power monitoring.

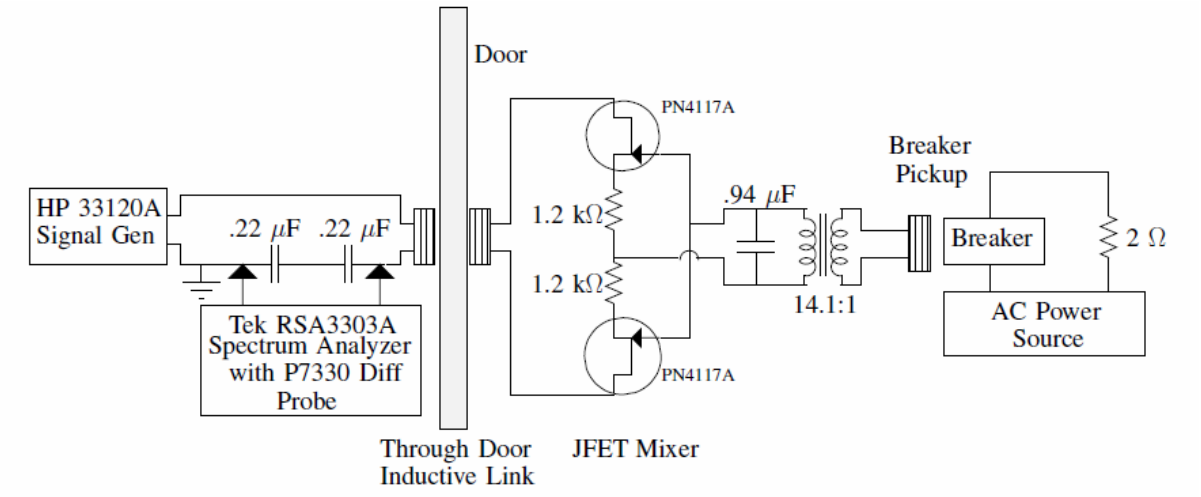

Figure 9: "Through Door" current sensor with no direct electrical contact.

Ansoft's Maxwell 3D was used to model the magnetic fields generated by the current-carrying member inside a typical circuit breaker. The geometric model of the current-carrying member shown in Figure 8 was developed to match the geometry common to several brands of circuit breakers. The simulated magnetic fields were used to identify the appropriate location of the breaker pickup. Various breaker pickup shapes were considered to yield sufficient concentration of magnetic flux in the pickup core. Simulations using the finite element modeling software, FEMM, verified that a half toroid of high permeability material placed on the breaker face was suitable. A typical FEMM simulation is depicted in Figure 10.

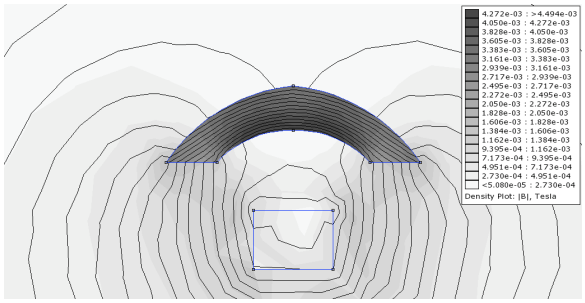

Figure 10: Finite Element Magnetic Model (FEMM) of magnetic flux through the breaker. The plastic breaker is ignored because it is neither conductive nor affected by the magnetic field.

To form the magnetic yoke, a core with relative permeability of 10,000 was first cut in half. The two halves were then joined for increased cross-sectional area. A total of 1,200 turns of 34 AWG magnet wire were wrapped around the yoke. A photograph of the breaker pickup on the breaker face is shown in Figure 11. Maximizing the number of turns, cross-sectional area and relative permeability was important for increasing the inductance of the breaker pickup. The resulting inductive impedance at 60 Hz was sufficient to provide suitable voltage signals corresponding to the breaker current.

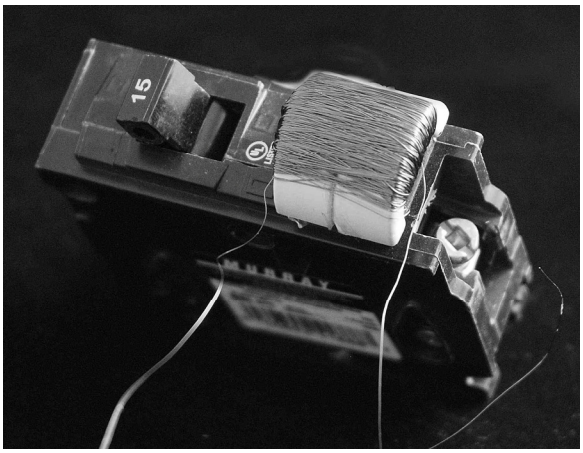

Figure 11: Breaker pickup

The four-quadrant balanced JFET modulator (mixer) implemented during our initial experiments, shown in Figure 12, was designed to transmit information from the breaker pickup through the inductive link and out of the breaker panel. This circuit consists of two JFET devices for modulation control and two resistors to improve linearity, but it does not require a DC power supply.

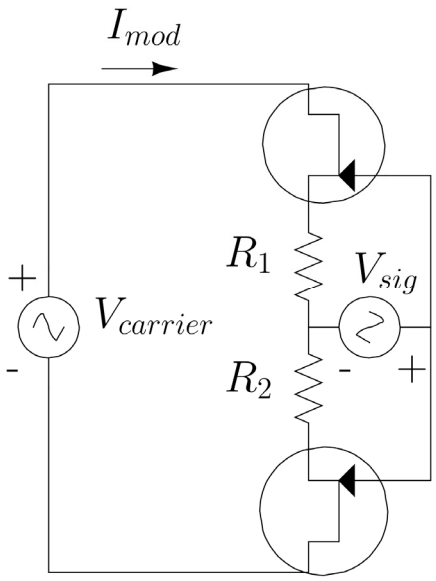

Figure 12: Adaptive Referencing Balanced two-JFET Modulator circuit enables simultaneous powering and modulation with no DC bus.

The power front-end, shown in Figure 13, is a push-pull driver composed of two BJT devices. The bases of these BJT devices are driven using a high voltage decompensated operational amplifier in a high gain configuration. A square wave at the carrier frequency is synthesized by the DSP and ac-coupled to the noninverting input of the amplifier. The operational amplifier then increases the voltage to a level suitable for driving the push-pull driver.

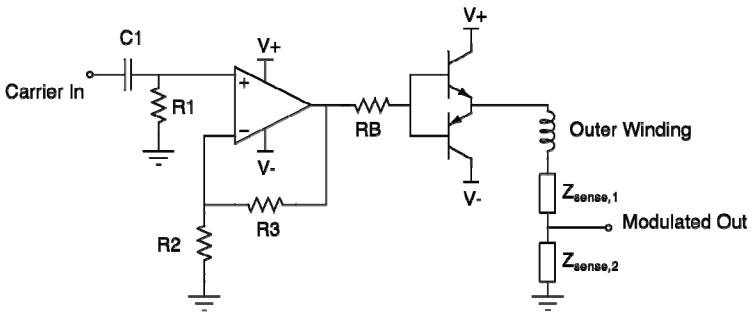

Figure 13: A simplified schematic of the coil drive power front-end.

The push-pull driver is connected to the series combination of the outer coil and two sense impedances. The voltage between the two sense impedances is taken as the input to the analog filter chain. The total sense impedance is matched to the coil impedance at the carrier frequency, but the ratio of the two impedances is chosen to deliver acceptable voltage levels to the analog signal chain.

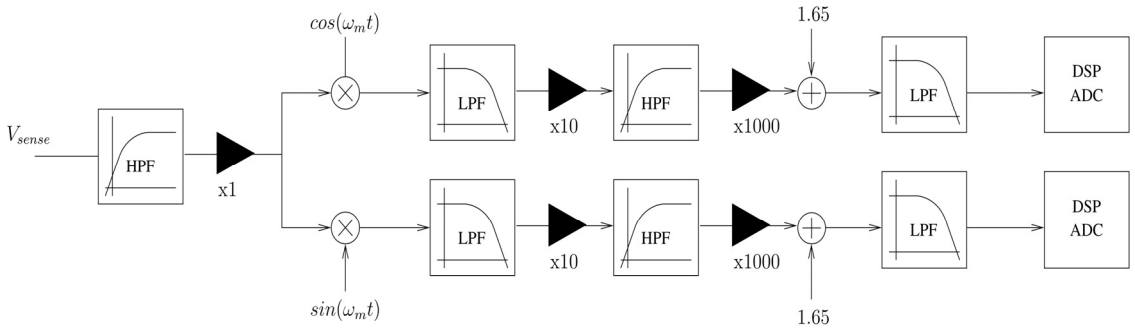

Figure 14: Block diagram of analog filter chain

The test signal generator and spectrum analyzer shown in Figure 9 have been replaced with custom circuitry that could serve as a beginning for a standalone sensor that could be commercialized. A block diagram of the analog signal chain is shown in Figure 14. The analog front end measures the voltage across the coil sense impedance, V_{sense}. In-phase and quadrature reference signals multiply the measured signal resulting in the *I* and *Q* channels shown. Multiplication is achieved with a full-bridge consisting of analog switches. The demodulated signal is followed by a low-pass filter that attenuates the remaining high frequency content. While the signal of interest is demodulated to 60 Hz, the unsuppressed carrier in the input signal is demodulated to dc. Removing the resulting dc offset with a highpass filter allows for a large gain before sampling. A final low-pass filter reduces aliasing in the sampled signal, while an offset of 1.65 V centers the signal in the input voltage range of the 12-bit ADC. The *I* and *Q* channels are combined using a dsPIC33 to form the final output signal. Here, we discuss some tradeoffs in various demodulation techniques while highlighting those used in our experimental setup.

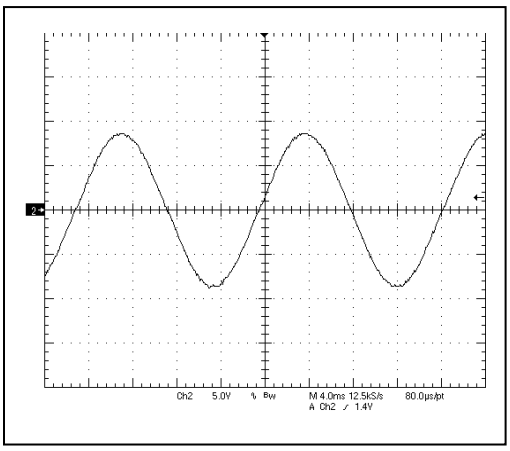

(a)

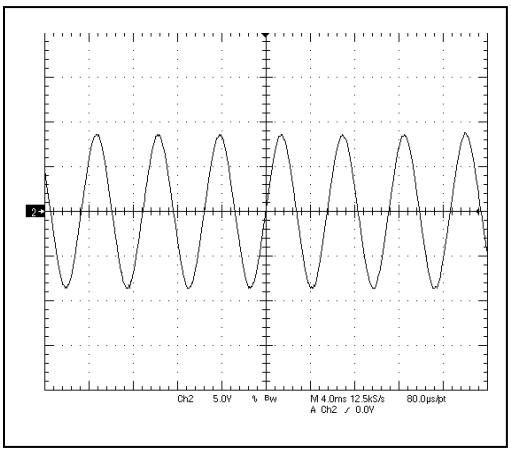

(b)

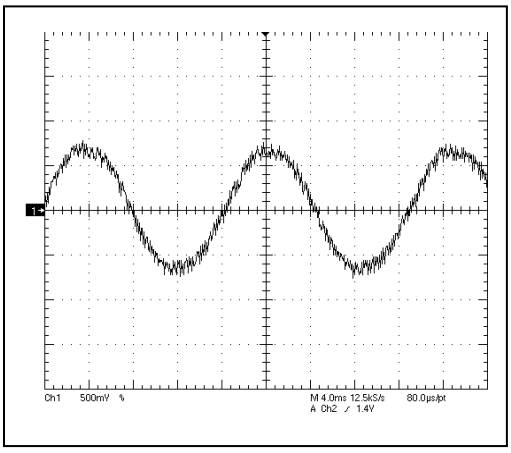

(c)

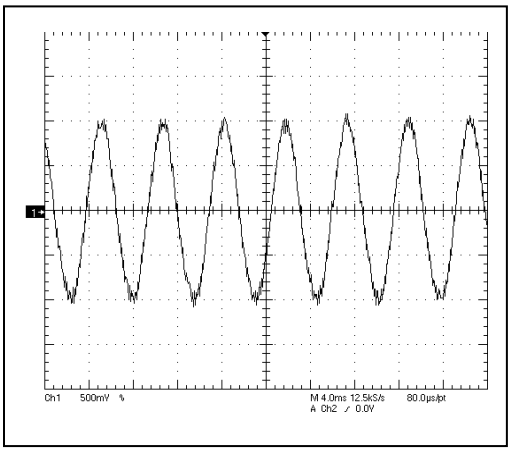

(d)

Figure 15: (a) and (b): Breaker currents generated for testing, (c) and (d): demodulated signals corresponding to the breaker currents in (a) and (b).

Figure 15 shows successful results from our field testing. The top graphs, (a) and (b) in Figure 15, show two different currents in the main breaker under observation. The bottom graphs, (c) and (d) in Figure 15, show the reconstructed currents using our test coil and circuitry.

1.3 Retrofit Acoustic Water Sensor

A pipe distribution network, e.g., for water or gas utilities, in a building can not only deliver a commodity like water but can also serve as it's own sensor for monitoring water flow and the operation of individual water consuming appliances. We have demonstrated technology that permits nonintrusive monitoring of water consumption and the identification of the operation of individual water consuming loads like dishwashers and clothes washers from nonintrusive measurements. These measurements of water consumption can be correlated with nonintrusive measurements of electrical consumption for "one stop" monitoring of all utility consumption in a building from a single nonintrusive metering installation.

From a single non-intrusive acoustic sensor attached at the point of aggregate water intake to a building, it is possible to monitor the turn-on and shut-off transient frequency signatures of water fixtures and appliances in the building. These signatures can be identified by a software system, which can processes the data and identifies the loads. Here, we show experimental data from deployment of a prototype system in a single-family home. The results from this data demonstrate that individual loads on the system are identifiable from a single non-intrusive monitoring point, and that individual loads remain identifiable and distinguishable even when multiple loads are in use.

Preliminary data for analysis was collected using a single non-intrusive acoustic sensor at the point of aggregate water intake for the building. For the prototype system, the acoustic sensor consisted of a microphone encased in a foam block to dampen ambient sound.

Figure 16. Microphone

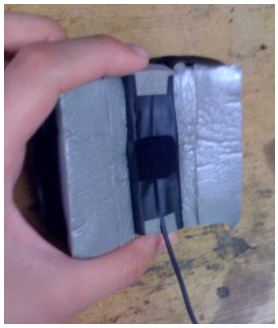

Figure 17. Foam block assembly

Figure 18. Mounted assembly

The assembly was fastened to the outside of the aggregate water intake pipe to a single family home. This pipe was located in the basement of the house. The home water supply pipe network is illustrated schematically in Figure 19.

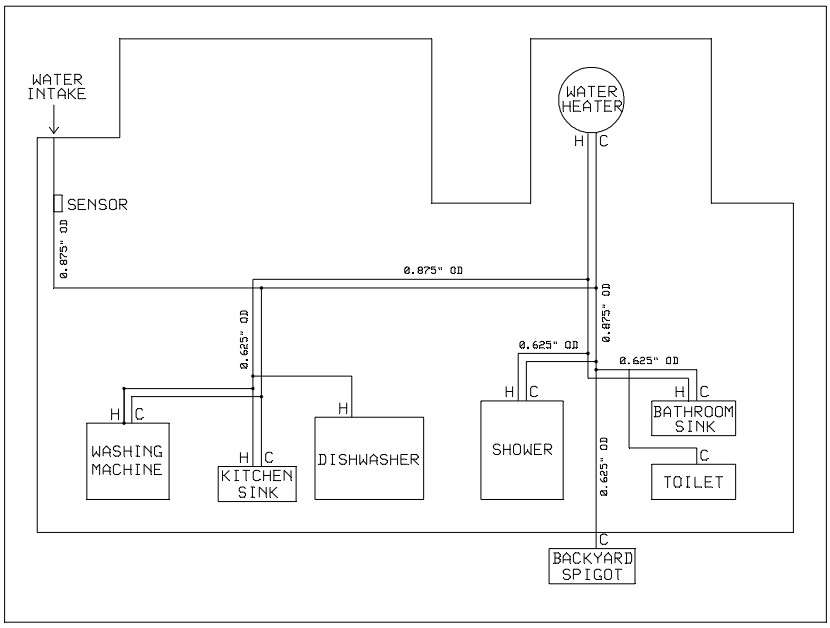

Figure 19. Diagram of field test site

There are many different water consuming loads on the pipe network, including a toilet, shower, and sinks, as well as appliances such as a dishwasher and a washing machine.

The energy spectral density of acoustic noises on the plumbing system has distinct frequency peaks. In essence, the plumbing is a kind of musical instrument with a distinct set of "notes" or frequency signatures. Different notes and combinations of notes are associated with the operation of individual loads on the system. These signatures can be learned and disaggregated from the acoustic measurement, even when several loads are operating at the same time. The acoustic information can be processed using signal processing algorithms based in the physics of the hydrodynamic flow in order to separate or disaggregate individual load operation when multiple loads are operating, and in the face of pressure changes in the system. Figure 20 illustrates typical data that we have observed in the field, and shows that characteristic signatures for different water appliances can be found even when multiple loads operate at the same time.

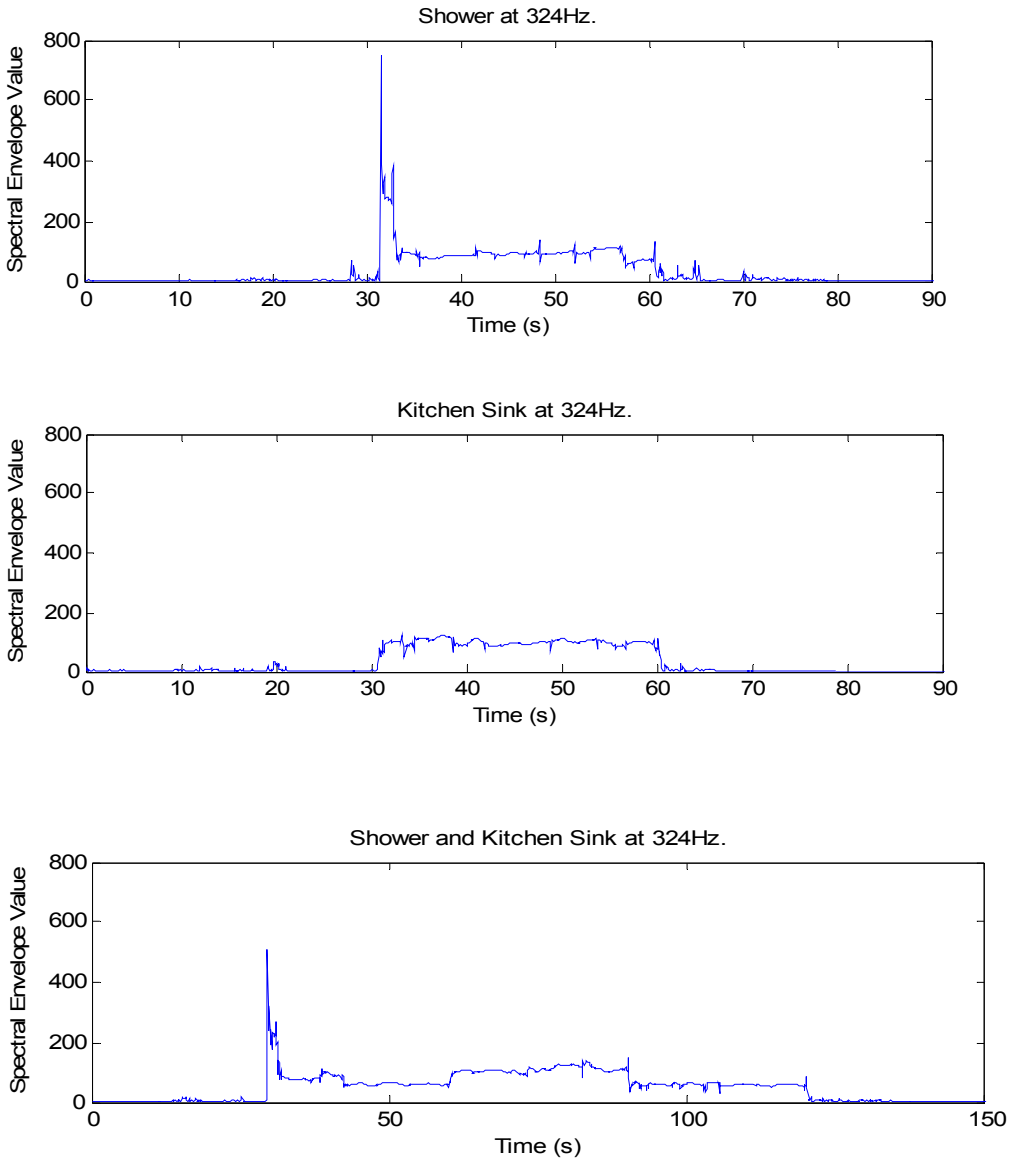

Figure 20: Acoustic frequency content recorded during operation of a shower (top graph), a sink (middle graph), and a combination of both, where the sink is activated during the middle of a shower run (lower graph).

2. Electrostatic Proximity Detection

Sponsors
U.S. Department of Energy
The Grainger Foundation
MIT Energy Initiative

Project Staff
J.J. Cooley, D.R. Vickery, A. Avestruz, and S. Leeb

We have demonstrated that light fixtures like fluorescent or solid-state lamps can be used as proximity sensors to detect people. People have dielectric properties that disturb the electric fields around fluorescent lamps. The dielectric properties of people are available as a sensor target even when people are sedentary or motionless, in contrast to typical PIR sensors, for example. The dielectric properties of people make a measurable disturbance in the electric fields around lamps, including both fluorescent and solid state fixtures, as shown in the three electric field simulations around a fluorescent lamp, below.

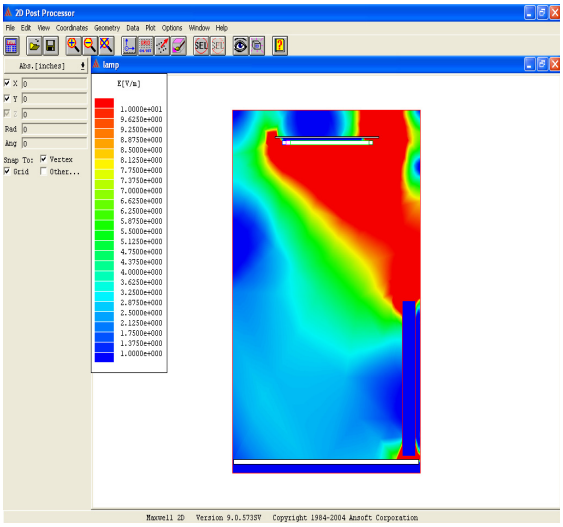
2D Post Processor
lamp
E[V/m]
Maxwell 2D Version 9.0.5735V Copyright 1984-2004 Ansoft Corporation

Lamp

←

←

"Person"

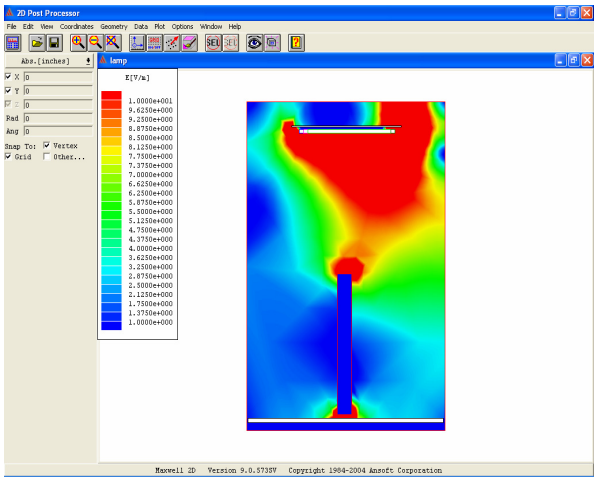
2D Post Processor
lamp
E[V/m]
Maxwell 2D Version 9.0.5735V Copyright 1984-2004 Ansoft Corporation

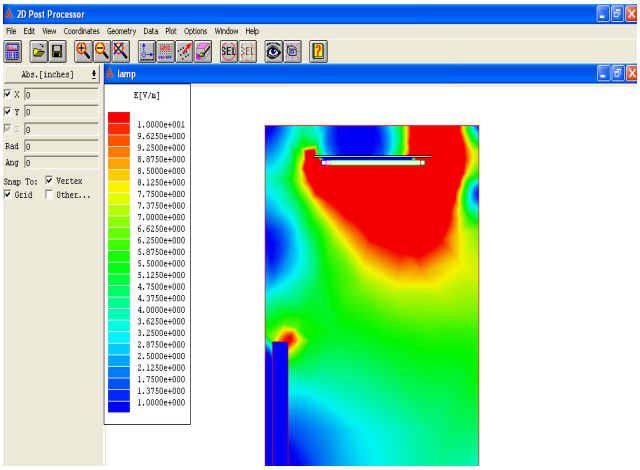
2D Post Processor
lamp
E[V/m]

These three plots show the electric field intensity around a fluorescent lamp fixture as a columnar "person" moves under the lamp. The field intensity is indicated by the colors or shading in the pictures. The changes in the field patterns can be detected by electronics that can be co-located in the solid-state lamp ballast. Information about the presence or absence of occupants, time of day, and other information like sensed day light from a photocell in the ballast can be used to locally control the operation of the lamp.

These electric field disturbances can be used to detect the presence of people, and they permit our demonstration fixture to automatically detect people by their dielectric presence regardless of whether or not they are moving. We have demonstrated detection ranges of 10-15 feet, and can increase this for different luminaries and mounting locations. An array of lamps in a room can be used to create a broad area tracking system.

A fluorescent bulb can be treated as an AC line current that radiates electric fields. If the fluorescent bulb is treated as a transmitter, and a metallic electrode in front of the bulb is treated as a receiver, the capacitive coupling between the two results in an AC current from the transmitter to the receiver. This current can then be sensed and amplified. When a conducting body such as a person or metallic object in the vicinity of the electric fields, capacitive coupling from the transmitter to the body and from the body to ground redirects some of the current away from the receiving electrode and into ground. By measuring the reduction in current at the receiver, the amount of person or conducting body under the lamp is deduced. Furthermore, by using more than one electrode and comparing measurements at each electrode, the location of the body and even motion of the body under the lamp is deduced.

The model of the lamp and loading body developed during the proposed effort has lead to a lumped circuit model. The model consists of capacitances between the transmitter, receiver, the loading body, and ground. Approximate values for these capacitances are obtained from modeling and from calculations. These values are used in the design of the receiving circuitry and can be used to place realistic bounds on the detection range. They may support more advanced "imaging" applications to provide more detailed portraits of occupancy.

Our prototype hardware configuration contains of three primary electronic subsystems: a dimming fluorescent lamp ballast, a sensor that contains all the analog and digital electronics for acquiring and processing sensor data, and a power supply for the isolating the ballast and powering the sensor. A block diagram of this system is shown in below.

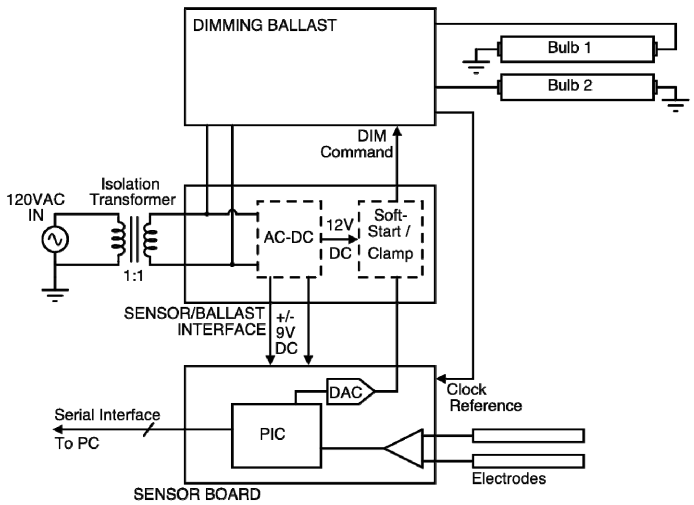

A block diagram of the three-board lamp sensor system: Dimming Ballast, Sensor Board, and Interface.

The ballast can be automatically dim and brighten lighting as people move through a building. In sparsely populated areas, a person travels in a "pool" of light. We are also developing ballasts that modulate the arc in a lamp, permitting the lamp to transmit information optically while retaining conventional illumination capability.

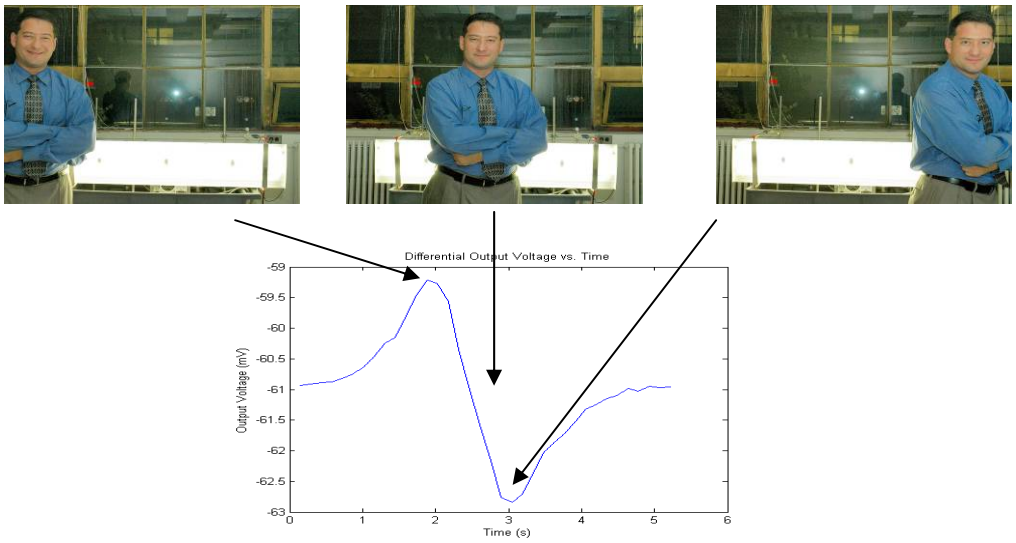

Proximity sensing

Publications

Journal Articles, Published

Mitchell, G.R., R.W. Cox, J. Paris, S.B. Leeb, "Shipboard Fluid System Diagnostic Indicators Using Non-Intrusive Load," *Naval Engineer's Journal, Volume 119, No. 1*, November, 2007.

Shaw, S.R., S.B. Leeb, L.K. Norford, R.W. Cox, "Nonintrusive Load Monitoring and Diagnostics in Power Systems," *IEEE Transactions on Instrumentation and Measurement, Volume 57, No. 7, July 2008, pp. 1445-1454.*

Wichakool, W., A. Avestruz, R.W. Cox, S.B. Leeb, "Modeling and Estimating Current Harmonics of Variable Electronic Loads," *IEEE Transactions on Power Electronics, Special Issue, Volume 24, No. 12,* December, 2009, pp. 2803-2811.

Conference Articles, Published

Laughman, C.R., R. LaFoy, W. Wichakool, P. Armstrong, S.B. Leeb, et.al., "Electrical and Mechanical Methods for Detecting Liquid Slugging in Reciprocating Compressors," *International Compressor Engineering Conference,* Purdue University, West Lafayette, IN, C1437, July 14-17 2008.

Cooley, J.J., A. Avestruz, S.B. Leeb, "An Autonomous Distributed Demand-side Energy Management Network Using Fluorescent Lamps," *IEEE Power Electronics Specialists Conference*, Rhodes, Greece, June 2008.

Proper, E., Cox, R., Leeb, S., Douglas, K., Paris, J., Wichakool, W., Foulks, L., Jones, R., Branch, P., Fuller, A., Leghorn, J., Elkins, G., "Field Demonstration of a Real-Time Non-Intrusive Monitoring System for Condition-Based Maintenance," *Electric Ship Design Symposium*, National Harbor, Maryland, February 2009.

Paris, J., Remscrim, Z., Douglas, K., Leeb, S., et. al., "Scalability of Non-Intrusive Load Monitoring for Shipboard Applications," ASNE Day 2009, National Harbor, Maryland, April, 2009.

Laughman, C.R., Leeb, S.B., Norford, L.K., Shaw, S.R., Armstrong, P.R., "A Two-Step Method for Estimating the Parameters of Induction Machine Models," *IEEE Energy Conversion Conference and Exposition,* San Jose, CA, September 2009.

Clifford, Z., Cooley, J., Avestruz, A., Remscrim, Z., Vickery, D., Leeb, S.B., "A Retrofit 60 Hz Current Sensor for Non-intrusive Power Monitoring at the Circuit Breaker," *Applied Power Electronics Conference,* Palm Springs, CA, February, 2010.

Orji, U., Remscrim, Z., Laughman, C., Leeb, S.B., Wichakool, W., Schantz, C., Cox, R., Paris, J., Kirtley, J.L., Norford, L.K., "Fault Detection and Diagnostics for Non-Intrusive Monitoring using Motor Harmonics," *Applied Power Electronics Conference,* Palm Springs, CA, February, 2010.

Remscrim, Z., Paris, J., Leeb, S.B., Shaw, S.R., Neuman, S., Schantz, C., Muller, S., Page, S., "FPGA-Based Spectral Envelope Preprocessor for Power Monitoring and Control," *Applied Power Electronics Conference,* Palm Springs, CA, February, 2010.

Wichakool, W, Paris, J., Avestruz, A., Leeb, S.B., "High-resolution Physically-windowed Sensors for Power Electronics Applications," *Applied Power Electronics Conference,* Palm Springs, CA, February, 2010.

Cooley, J.J., Seger, E., Leeb, S.B., Shaw, S., "Characterization of a 5 kW Solid Oxide Fuel Cell Stack Using Power Electronic Excitation," *Applied Power Electronics Conference,* Palm Springs, CA, February, 2010.

Cooley, J.J., Vickery, D., Avestruz, A., Englehart, A., Paris, J., Leeb, S.B., "Solid-State Lamp with Integral Occupancy Sensor," *Applied Power Electronics Conference,* Palm Springs, CA, February, 2010.